Molecular Therapy
Methods & Clinical Development
Original Article

An AAV capsid increases transduction of striatum and a ChAT promoter allows selective cholinergic neuron transduction

Miguel C. Santoscoy,[1,2,3] Paula Espinoza,[1,2,3] Demitri De La Cruz,[1,2,3] Mohammed Mahamdeh,[1,4] Jacqueline R. Starr,[1,5] Nikita Patel,[1,2,3] and Casey A. Maguire[1,2,3]

[1]Harvard Medical School, Boston, MA, USA; [2]Department of Neurology, Massachusetts General Hospital, Boston, MA, USA; [3]Molecular Neurogenetics Unit, Massachusetts General Hospital, Charlestown, MA, USA; [4]Cardiovascular Research Center, Massachusetts General Hospital, Charlestown, MA, USA; [5]Channing Division of Network Medicine, Brigham and Women's Hospital, Boston, MA, USA

Adeno-associated virus (AAV) vectors are currently the most efficient option for intracranial gene therapies to treat neurodegenerative disease. Increased efficacy and safety will depend upon robust and specific expression of therapeutic genes into target cell-types within the human brain. In this study, we set out with two objectives: (1) to identify capsids with broader transduction of the striatum upon intracranial injection in mice and (2) to test a truncated human choline acetyltransferase (ChAT) promoter that would allow efficient and selective transduction of cholinergic neurons. We compared AAV9 and an engineered capsid, AAV-S, to mediate widespread reporter gene expression throughout the striatum. We observed that AAV-S transduced a significantly greater area of the injected hemisphere primarily in the rostral direction compared with AAV9 (CAG promoter). We tested AAV9 vectors packaging a reporter gene expression cassette driven by either the ChAT or CAG promoter. Specificity of transgene expression of ChAT neurons over other cells was 7-fold higher, and efficiency was 3-fold higher for the ChAT promoter compared with the CAG promoter. The AAV-ChAT transgene expression cassette should be a useful tool for the study of cholinergic neurons in mice, and the broader transduction area of AAV-S warrants further evaluation of this capsid.

INTRODUCTION

The clinical potential of gene therapy to treat a wide range of human diseases *in vivo* has been shown mainly by utilizing adeno-associated virus (AAV) vectors. Currently there are six AAV-based gene therapies approved by the Food and Drug Administration in the United States or the European Medicines Agency (EMA) for the treatment of deadly diseases such as spinal muscular atrophy[1] and diseases of high morbidity such as hemophilia A[2] and B (fda.gov) and Leber's congenital amaurosis.[3] These approved therapies and hundreds more in trials demonstrate the clinical relevance of AAV vectors and the major progress made in the field over the past 3 decades.

Neurological disorders are one of the most pressing diseases. Thus, AAV vectors that allow robust transduction of desired target cells in the central nervous system (CNS) will contribute to improve clinical outcomes in patients. In 2022, an AAV2-based medicine, Upstaza, for the treatment of severe aromatic L-amino acid decarboxylase deficiency by direct intra-striatal injection, was approved by the EMA.[4] The striatum is one of the main input structures for the basal ganglia. Due to its large volume, cellular composition, inputs and outputs with other brain structures, and architecture, the striatum plays a major role for movement[5] and cognition.[6] Alterations of the abundance or the functionality of striatal neurons can lead to several neurological diseases including Parkinson's and Alzheimer's disease.[7] The most abundant striatal neurons are GABAergic medium spiny neurons (MSNs) making up 90% of all neurons in this structure.[8] Despite their low abundance in the striatum (1%–3%), cholinergic neurons regulate MSN activity and fine-tune a variety of brain functions.[9] Thus, strategies for increasing AAV transduction specificity and efficiency toward striatal MSNs and cholinergic neurons will contribute to develop therapies for rewiring neuronal disorders after intracranial administration.

Despite clinical efficacy with intracranially injected AAV, several improvements are still needed to optimize the system involving both the capsid and transgene expression cassette. First, direct intraparenchymal injection of AAV vectors via burr holes drilled into the skull is an invasive procedure. Because of limited diffusion of AAV from the injection site, for large brains in humans, multiple burr holes must be drilled and multiple injections performed to get sufficient "coverage" of transduced cells in the striatum. Obtaining capsids that spread a greater distance in the striatum is highly desirable to reduce the number of required injections and potential complications that result. Second, for some neuronal subtypes, such as cholinergic neurons, conventional broadly active promoters such as CMV or CAG placed in AAV or adenovirus vectors are not very efficient or specific at transgene expression.[10,11] Cholinergic neurons express choline acetyltransferase (ChAT) required to produce the neurotransmitter acetylcholine. Prior studies using the

Received 13 January 2023; accepted 4 May 2023;
https://doi.org/10.1016/j.omtm.2023.05.001.

Correspondence: Casey A. Maguire, Harvard Medical School, Boston, MA, USA.
E-mail: cmaguire@mgh.harvard.edu

ChAT promoter to drive transgene expression in transgenic mice have resulted in selective expression in cholinergic neurons.[12,13] More recently Martel et al. used a canine adenovirus vector packaging a ChAT-promoter-driven transgene cassette, yielding transduction of ChAT neurons in rat and NHP striatum.[11]

Here, we attempted to address the aforementioned challenges faced by AAV vector-mediated transduction of striatum, enhanced transduced striatum area, as well as improved efficiency and selectivity of cholinergic neurons using a novel engineered AAV capsid and a truncated human ChAT promoter, respectively.

RESULTS

Intracranially injected AAV9 and AAV-S mediate robust transduction with enhanced spread of transduced area with AAV-S

Transduction of striatal neurons is desired for the development of gene therapies targeting neuronal degeneration that often affects this brain region. To attempt to identify a capsid with broad transduction throughout the striatum, we tested our recently described AAV-S capsid.[14,15] In earlier studies, we noticed this capsid gave robust transduction of the brain after intra-cortical and intra-hippocampal injection.[14] We performed a direct comparison of AAV-S to its parental capsid AAV9 using a CAG-tdTomato expression cassette (Figures 1A and 1B). Adult C57BL/6 mice (n = 3) were injected into the striatum with 1.3 x 10^{10} vg of either capsid, and 2 weeks later, brains were harvested and cryosections imaged for intrinsic tdTomato fluorescence using epifluorescence microscopy. For both capsids, we observed intense tdTomato expression visible to the naked eye in natural light around the injection site in harvested brains (Figure 1C). To measure transduction across the striatum, we analyzed the transduced region of the injected hemisphere spanning 1.5 mm on either side of the bregma (Figure 1D). Coronal sections were made spanning the injection site and epifluorescence microscopy performed to visualize AAV-mediated tdTomato intrinsic fluorescence. For both capsids, we observed robust tdTomato expression in the ipsilateral hemisphere (Figure 1E). We performed image analysis for three C57BL/6 mice per vector, to quantify the transduced area of each hemisphere at nine regions spanning the injection site. Interestingly, AAV-S transduced a higher area of the injected hemisphere compared with AAV9 (two-way ANOVA, $p < 0.0001$, Figure 1F). The difference was greatest in the three most rostral sections in which AAV-S transduced 1.8- to 3.2-fold larger areas of injected hemisphere than AAV9 (Figure 1F). For AAV-S, we noticed that transduction in the far rostral region displayed a mottled/blotchy pattern extending into the insular cortex (Figures 1E and S1). This is reminiscent of anterograde or retrograde transduction of distal neurons by AAV, which may help explain some of the increased spread observed with AAV-S compared with AAV9.

As most striatal neurons are MSNs, we stained sections for DARPP32, which is specific for this cell type, and we observed abundant DARPP32 signal colocalization with transgene expression for both capsids (Figure 1G).

Direct intracranial injection of AAV9 with ChAT promoter transduces cholinergic neurons selectively and efficiently

In an unpublished study, we observed that the majority of transduced cells after intracranial injection of AAV vectors using a broadly active CAG promoter were not cholinergic neurons. To improve both specificity and efficiency of cholinergic neuron transduction, we engineered an AAV expression plasmid that contains a region of the ChAT promoter previously shown to have transcriptional activity[16] (Figure S2). We named this plasmid pAAV-ChAT-tdTomato. Next, we produced AAV9 vectors packaging either AAV-CAG-tdTomato or AAV-ChAT-tdTomato (Figure 2A). The transgenic mouse strain ChAT(BAC)-eGFP was used to identify striatal cholinergic neurons (Figure 2B). Mice were injected with 2.5 x 10^9 vg/animal in the striatum with either vector. To avoid spectral overlap of tdTomato into the GFP fluorescence spectrum, we reduced the dose of vector compared with Figure 1 by 5-fold, which allowed accurate identification of cholinergic (GFP+) neurons. 16 days post injection, we harvested brains, and performed sectioning, confocal microscopy with z stack analyses, and semi-automated quantification of transduced cells. Brain sections from mice injected with AAV9-CAG-tdTomato (n = 3) showed robust transduction of many GFP-negative cells in the striatum, with some transduction of GFP-positive cholinergic neurons (Figure 2C). On the other hand, brains from mice injected with AAV9-ChAT-tdTomato (n = 2) displayed a transduction pattern in far fewer GFP-negative cells and with higher colocalization percentage with GFP-positive cholinergic neurons (Figures 2C and 2D). To quantitate these results, we measured the efficiency and specificity of transduction by image analysis. We focused on sections immediately proximal to the injection site (i.e., this was not a measure of transduction spread as done in Figure 1). Specificity was defined as the number of transduced (tdTomato positive) cholinergic neurons over the total number of transduced cells (both GFP-positive and -negative cells). Efficiency was defined as the number of cholinergic neurons (GFP) that co-localized with vector-mediated tdTomato expression over the total number of cholinergic neurons in the entire injected striatum. We found that AAV9-ChAT-tdTomato specificity was 64% compared with only 8.9% for the same capsid with the AAV-CAG-tdTomato expression cassette (unpaired t test, $p = 0.01$, Figure 2E). Efficiency trended higher with the ChAT promoter, yielding 42% of cholinergic neurons in the entire striatum being transduced compared with 14.2% with the CAG promoter (unpaired t test, $p = 0.0551$, not significant, Figure 2F).

AAV-S-ChAT-tdTomato also transduces cholinergic neurons, with slightly lower specificity than AAV9 near the injection site

To understand if AAV-S capsid would alter either the efficiency or specificity of cholinergic neuron transduction compared with AAV9 when using the ChAT-promoter-driven tdTomato cassette, ChAT(BAC)-eGFP mice were injected into the striatum with 2.5 x 10^9 vg/animal (n = 2) of AAV-S-ChAT-tdTomato, and 16 days later, brains were harvested for image analysis as before (Figures 3A and 3B). We compared the transduction specificity and efficiency of AAV-S-ChAT-tdTomato with that of AAV9-ChAT-tdTomato

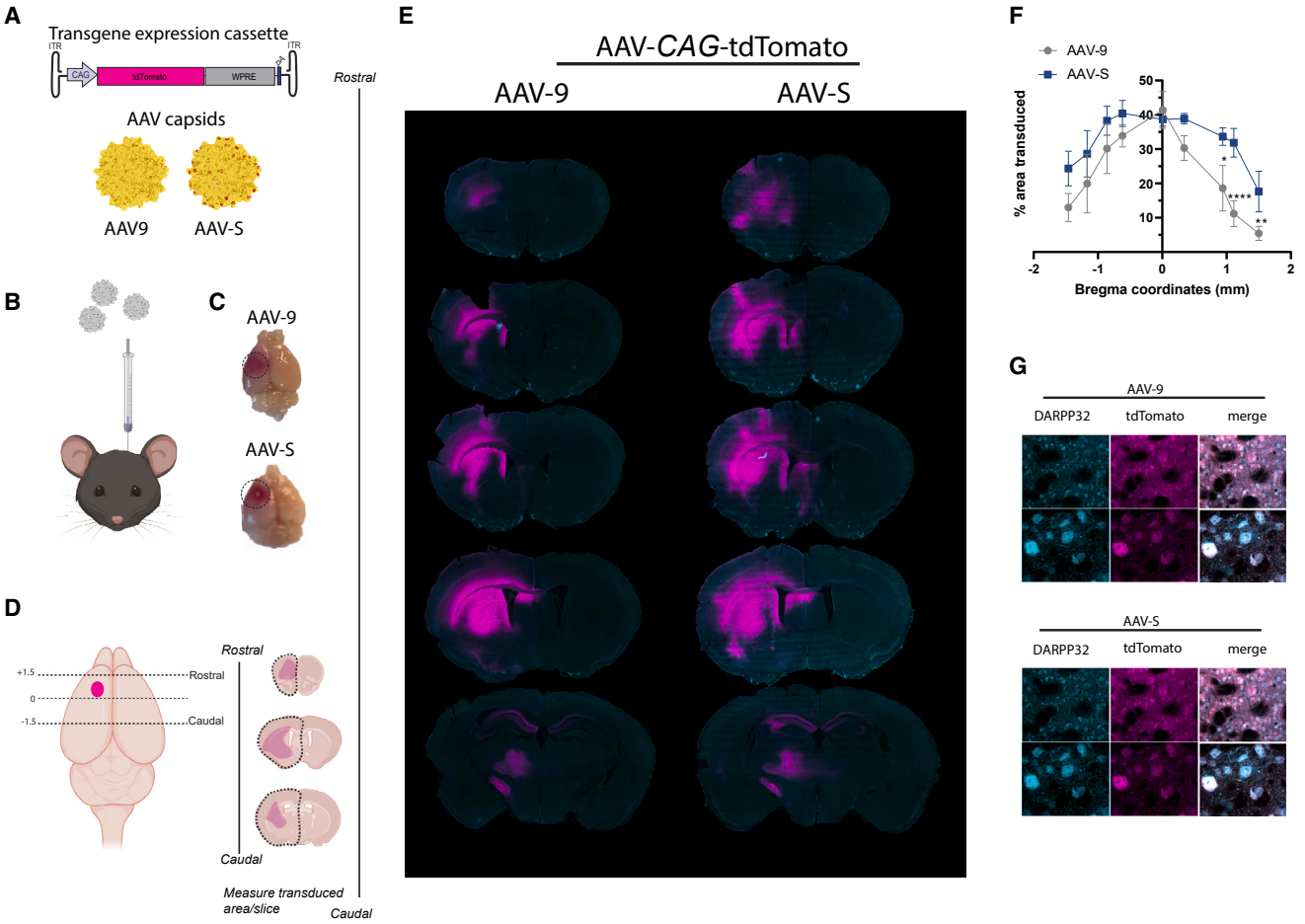

Figure 1. AAV-S transduces a greater area of striatum than AAV9 after direct injection in C57BL/6 mice

(A) AAV transgene expression cassette and capsids used in these experiments. The AAV expression plasmid is a single-stranded genome. CAG promoter is composed of the following: CMV early enhancer element, the chicken beta actin (CBA) promoter, the first exon and intron of CBA gene, and the splice acceptor from the rabbit beta-globin gene. ITR, inverted terminal repeats; WPRE, woodchuck hepatitis virus post-transcriptional regulatory element; pA, SV40 polyadenylation signal. AAV capsids used are AAV9 and AAV-S. AAV-S contains a 7-mer sequence at the 3-fold axis of symmetry indicate by the orange dots. (B) C57BL/6 female mice (n = 3/capsid) were stereotactically injected into the striatum with 1.3×10^{10} vg/animal of either vector. 2 weeks later, brains were harvested to assess transduction (tdTomato fluorescence). (C) A representative brain injected with AAV9 and AAV-S showing visible red-tdTomato protein expression around the injection site (dashed circle). (D) Brain sections were analyzed for rostral to caudal spread of transduction by AAV9 and AAV-S. Left image: we spanned 3.0 mm around the bregma including the injection site (magenta dot). Right image: coronal sections on the injected hemisphere were measured for the percentage that was tdTomato positive using imaging analysis software. (E) Representative coronal sections from −1.5 to +1.5 caudal to rostral for mice injected with either capsid. TdTomato fluorescence is shown in magenta and DAPI staining in cyan. (F) Quantitation of transduced hemisphere transduction across different coordinates in the striatum for both capsids. A two-way ANOVA followed by a post hoc test for multiple comparisons was performed. *p = 0.035, **p = 0.005, ****p < 0.0001. Error bars represent the standard deviation from the mean. (G) AAV9 and AAV-S transduce medium spiny neurons as observed by DARPP32 staining (cyan) and tdTomato fluorescence (magenta). Top panels, low magnification; bottom panels, high magnification.

(same data generated from Figures 2E and 2F) (representative images Figure 3C). We analyzed sections immediately proximal to the injection site. From this analysis, AAV9 trended toward a specificity of 64% vs. 45% (t test, p = 0.2502, not significant) (Figure 3D) and trended slightly higher efficiency of 42% vs. 29% (t test, p = 0.316, not significant) compared with AAV-S (Figure 3E).

We also performed intra-striatal injections of C57BL/6 mice (n = 3/group) with AAV9-ChAT-tdTomato and AAV-S-ChAT-tdTomato and compared tdTomato expression profiles to those from mice injected with AAV9-CAG-tdTomato and AAV-S-CAG-tdTomato. Similar to the findings of the ChAT(BAC)-eGFP transgenic, we observed intense, dense transduction of cells in the striatum with either capsid packaging the CAG promoter and sparse transduction with either capsid packaging the ChAT promoter. The cells transduced with AAV9 or AAV-S with the ChAT promoter had larger cell bodies that appeared to be cholinergic neurons (Figure S3). Unfortunately, attempts at immunostaining with two commercially available anti-ChAT antibodies failed, so precise colocalization could not be performed.

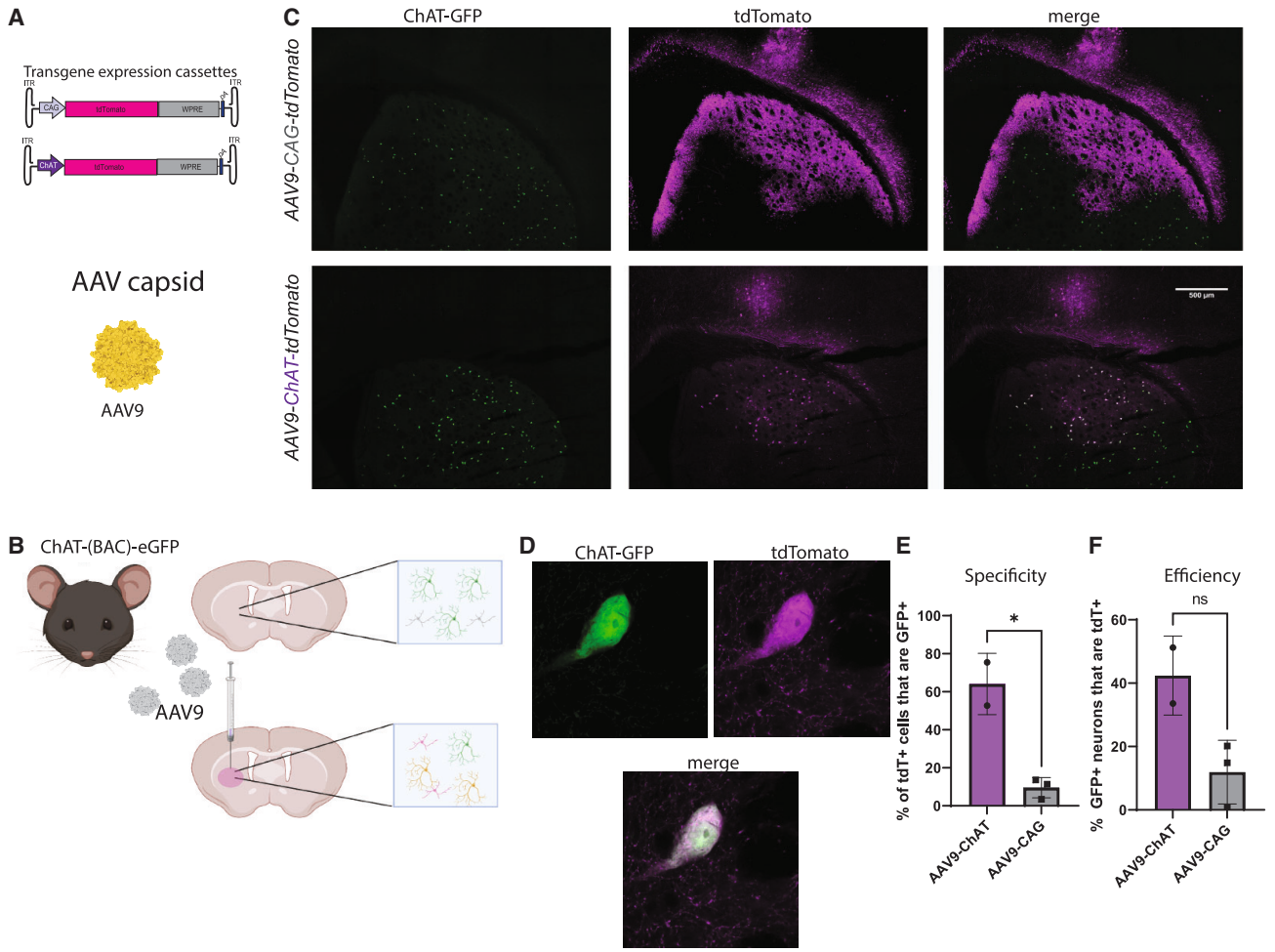

Figure 2. AAV9 transduction specificity and efficiency of cholinergic neurons in the striatum is increased using a ChAT promoter

(A) The AAV genomes containing either the CAG or the ChAT promoter driving tdTomato expression were packaged in the AAV-9 capsid for intracranial injection in mice. (B) Transgenic ChAT-GFP mice were stereotactically injected into the striatum with 2.5 x 10^9 vg/animal of the AAV9-CAG-tdTomato (n = 3) or AAV9-ChAT-tdTomato vectors (n = 2). (C) Representative images of the striatum indicate cholinergic neurons (ChAT-GFP, green color), transduced cells (tdTomato, magenta color), and transduced cholinergic neurons (merge). Scale bar represents 500 µm. (D) High (60x) magnification showing morphology of cholinergic neuron (GFP+) transduced by AAV9-ChAT-tdTomato. (E) Quantification of the selectivity of transduction (tdTomato+, GFP+ cells)/(total tdTomato+ cells) toward cholinergic neurons. An unpaired two-tailed t test was performed. *p = 0.01. Individual biological replicates are shown for each group in each bar graph. Error bars represent the standard deviation from the mean. (F) Efficiency of striatal cholinergic neuron transduction (tdTomato+, GFP+ cells)/(total GFP+ cells in the striatum) for each tested promoter. An unpaired two-tailed t test was performed. ns (not significant), p = 0.0551. Individual biological replicates are shown for each group in each bar graph. Error bars represent the standard deviation from the mean.

DISCUSSION

In this study we made two improvements to AAV-based gene transfer to the murine brain after direct injection. First, we showed greater AAV-S spread in the striatum than regular AAV9 after a single burr hole perforation in the skull. The striatum is the main port for input and output of neurochemical signals to maintain brain function, so several neurodegenerative diseases are associated with loss of striatal neuron circuits.[7] Due to the larger size of the human brain, the biodistribution of therapeutics requires multiple burr holes for intracranial injections into the brain parenchyma.[17] Thus, the ability of AAV vectors to spread within the striatum and CNS is highly desired. Nanoparticles, AAV, and other virus vectors spread via diffusion in the interstitial fluid of the extracellular matrix of the brain that is affected by particle diameter,[18] shape, and interactions with extracellular matrix components.[19] Infusion of vectors into the brain using convection-enhanced delivery increases the spread of vector using a slow positive pressure gradient (bulk flow).[20–22] Another way AAV vectors can spread beyond the injected area is via anterograde and retrograde transport along axons to transduce neuronal cell bodies in distal, connected brain regions.[23–25] AAV9 can mediate both anterograde and retrograde transport and transduction.[26] We noticed a mottled pattern of transduction with AAV-S in the most rostral regions of the brain sections examined (Figures 1E and S1) including in the insular cortex (IC). As the IC has been shown to project into

the striatum,[27] it is possible that AAV-S can retrogradely transduce IC neurons using their outputs to the striatum, perhaps with a greater efficiency than AAV9. Future studies will address this in detail, as it may be a useful mechanism to increase the transduced volume of brain after direct injections. The ability of AAV-S to spread through a larger area of the murine brain compared with AAV9 and the evidence of AAV-S transduction in the primate inner ear[15] motivate further testing with AAV-S in larger animals for the development of clinically translatable and less invasive therapies.

In addition to increased spread of transduction within the brain, we significantly increased AAV transduction selectivity and showed a trend toward greater efficiency of striatal cholinergic neurons *in vivo* by using the truncated human ChAT promoter.[16] The ChAT promoter showed 7-fold higher specificity of transduction of cholinergic neurons than the ubiquitous CAG promoter (Figure 2E) when using AAV9 capsid and a 3-fold increase the absolute number of transduced cholinergic neurons (Figure 2F). There was slight, yet not significant increases in specificity and efficiency of cholinergic neuron transduction with AAV9 over AAV-S (Figures 3D and 3E). The slight differences in specificity and efficiency between the capsids are unclear but may involve AAV-S having a higher tropism for non-cholinergic neuronal subtypes, yielding some off-target expression/leakiness of the ChAT promoter in those cells. The increased transduction specificity of cholinergic neurons due to transcription driven by the truncated ChAT promoter in mice supports previous observations of a study using adenovirus as vector and a truncated ChAT promoter in the striatum of rat and macaque monkey.[11] This prior work suggests that the AAV transgene expression cassette built for this study could also improve transduction of cholinergic neurons in larger animals and enhance the development of AAV vector research tools and therapies against neurological diseases due to the loss of density and function of cholinergic neurons such as Tourette syndrome or Parkinson's disease.[28–30]

Specificity of ~60% and transduction of 40% cholinergic neurons in the striatum using the AAV delivered ChAT promoter construct is a large improvement (7-fold and 3-fold, respectively) over the AAV-CAG construct and should be immediately useful to the neuroscience field. While our experiments in the ChAT(BAC)-eGFP transgenic mice used small group sizes of n = 2–3 mice, we are confident in the conclusion that AAV-ChAT-tdTomato is much more specific at cholinergic neuron transduction than AAV-CAG-tdTomato. First, there was a large difference that was statistically significant for specificity between the two groups (AAV9-CAG-tdTomato vs. AAV-ChAT-CAG-tdTomato) with low variability between animals in each group and no overlap in data points between groups (Figure 2E). Furthermore, we performed an independent experiment with n = 3 mice/group (Figure S3) and found, at a qualitative level, the same profound reduction in promiscuous transduction when using the AAV-ChAT-tdTomato construct vs. the AAV-CAG-tdTomato version.

Improvements can certainly be made to the AAV-ChAT promoter construct in the future to allow enhanced specificity and efficiency. These may include 3′ UTRs and enhancer elements of the ChAT gene. Also, the AAV inverted terminal repeats (ITRs) are known to possess transcription factor binding sites[31] that may drive low-level transcription in non-target cells at the high AAV genome copies observed with direct intracranial injections. Including ITR transcription insulating sequences before the ChAT promoter may reduce this if it is occurring. Furthermore data mining of miRNA sequences enriched in neuronal subtypes compared to cholinergic neurons may be used to incorporate the corresponding sequences into the AAV expression cassette to knock down transgene mRNA in these other neurons similar to what has been done with mIR183 de-targeting of AAV expression in dorsal root ganglion neurons but not neurons in brain or spinal cord.[32] Finally, identifying or engineering AAV capsids with more selective entry into cholinergic neurons may also increase specificity of transduction.

Regarding immediate useful applications of the different capsid/expression cassette combinations, we make the following suggestions: for applications in which broad transduction of striatal neurons is desired, the AAV-S capsid with the CAG promoter may be useful. In applications in which high specificity and efficiency for striatal cholinergic neurons is desired, the AAV9 capsid and ChAT promoter may be the best choice based on the comparisons made in this study. Overall, our findings support further development of the AAV-S capsid for transduction of brain and the AAV-ChAT promoter construct for cholinergic neuron transduction.

MATERIALS AND METHODS

Animals

All animal experiments were approved by the Massachusetts General Hospital Subcommittee on Research Animal Care following guidelines set forth by the National Institutes of Health Guide for the Care and Use of Laboratory Animals. We used adult age (8–10 week old) C57BL/6J (strain # 000664) and B6.Cg-Tg(RP23-268L19-EGFP) 2Mik/J (strain #007902) mice[12] (common name ChAT(BAC)-eGFP transgenic mice) all from The Jackson Laboratory, Bar Harbor, ME.

AAV vector production, purification, and titration

For transgene expression studies with AAV vectors, we used the following AAV expression plasmids: (1) pAAV-CAG-tdTomato (codon diversified) was a gift from Edward Boyden (Addgene plasmid # 59462; http://n2t.net/addgene:59462; RRID:Addgene_59462). This plasmid contains AAV ITRs flanking the CAG expression cassette, which consists of a hybrid CMV-IE enhancer/chicken β-actin (CBA) promoter, tdTomato cDNA, a woodchuck hepatitis virus post-translational response element (WPRE), and an SV40 poly A signal sequence. (2) pAAV-hChAT-tdTomato (codon diversified). To construct pAAV-hChAT-tdTomato, we utilized pAAV-CAG-tdTomato as backbone after removal of the CAG promoter using NdeI and KpnI (New England Biolabs, Ipswich, MA) restriction enzymes. Next, we ordered a gBlock double stranded DNA fragment from Integrated DNA Technologies (IDT, Coralville, Iowa) that contains an 894-bp fragment of the human ChAT promoter

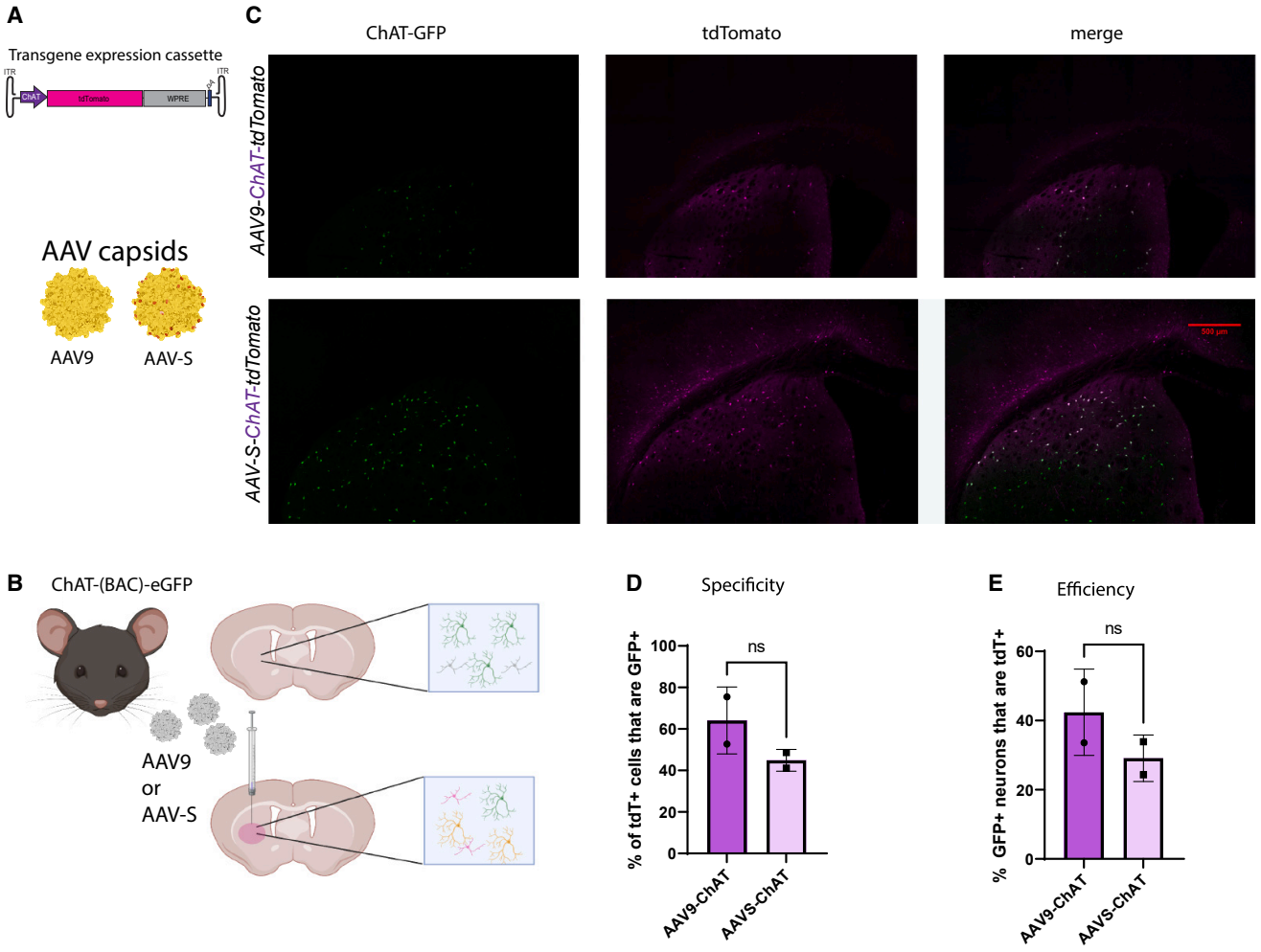

Figure 3. AAV-S-ChAT-tdTomato mediates slightly lower selectivity than AAV9 for cholinergic neurons near the injection site

(A) The AAV genome containing the truncated human ChAT promoter driving the expression of tdTomato was packaged into the AAV-9 and AAV-S capsids. (B) Transgenic ChAT-GFP mice (n = 2/capsid) were stereotactically injected with either AAV9 or AAV-S at 2.5 x 10^9 vg/animal. (C) Representative confocal microscopy images of the striatum of transgenic mice injected with either AAV9-ChAT-tdTomato or AAV-S-ChAT-tdTomato. Scale bar represents 500 µm. Cholinergic neurons (ChAT-GFP) are shown in green, transduced cells (tdTomato) are shown in magenta, and co-localized cells (merge) indicate transduced cholinergic neurons using AAV-ChAT-tdTomato genome. (D) Quantification of transduction specificity. An unpaired two-tailed t test was performed. Not significant, ns, p = 0.25. Individual biological replicates are shown for each group in each bar graph. Error bars represent the standard deviation from the mean. (E) Quantification of transduction efficiency. The same numbers for AAV9-ChAT-tdTomato used for Figure 2 were used for the comparison to AAV-S-ChAT-tdTomato. An unpaired two-tailed t test was performed. ns, p = 0.32. Individual biological replicates are shown for each group in each bar graph. Error bars represent the standard deviation of the mean.

identified in Bausero et al.[16] (see Figure S2 for sequence information). The gBlock contained 30 bp of homology arms on both ends to allow Gibson Assembly (New England Biolabs, Ipswich, MA) into the digested pAAV-tdTomato plasmid in place of the CAG promoter. The resulting plasmid, pAAV-hChAT-tdTomato, was transformed into SURE electrocompetent *E. coli* (Agilent Technologies, Lexington, MA) at 1700 V. Single colonies were inoculated into 3 mL of Luria Bertani medium (Fisher Scientific) containing 100 mg/L ampicillin, and cells were grown at 37°C and 250 rpm for 16 h. Plasmid was extracted utilizing the QIAprep Spin Miniprep Kit (250) (QIAGEN); the extracted plasmid was digested with SmaI restriction enzyme (New England Biolabs, Ipswich, MA) at room temperature for 1 h to confirm ITR integrity. The correct clones were sent for complete plasmid sequencing at PlasmidSaurus (Eugene, OR).

We used the following two capsids for these studies: AAV9 that was encoded in the pAR9 rep/cap vector kindly provided by Dr. Miguel Sena-Esteves at the University of Massachusetts Medical School (Worcester, MA). The AAV-S capsid is a previously described engineered AAV9-based capsid.[14,15] pAAV-S in pAR9 (rep/cap) is available at Addgene from Casey Maguire (Addgene plasmid # 174539; http://n2t.net/addgene:174539; RRID: Addgene_174539).

AAV production was performed as previously described.[33] Briefly, 293T cells were triple transfected using PEI MAX solution (Polysciences, Warrington, PA) with (1) AAV- rep/cap plasmid (either AAV-S or AAV9), (2) an adenovirus helper plasmid, pAdΔF6, and (3) ITR-flanked AAV transgene expression plasmid (either AAV-CAG-tdTomato or AAV-hChAT-tdTomato). Cell lysates were harvested 68–72 h post transfection and purified by ultracentrifugation of an iodixanol density gradient. Iodixanol was removed, and buffer was exchanged to phosphate buffered saline (PBS) containing 0.001% v/v Pluronic F68 (Gibco, Grand Island, NY) using 7-kDa molecular weight cutoff Zeba desalting columns (Thermo Scientific). Vector was concentrated using Amicon Ultra-2 100-kDa MWCO ultrafiltration devices (Millipore Sigma). Vector titers in vg/ml were determined by Taqman qPCR in an ABI Fast 7500 Real-time PCR system (Applied Biosystems) using probes and primers to the ITR sequence and interpolated from a standard curve made with a restriction enzyme linearized AAV plasmid. Vectors were pipetted into single-use aliquots and stored at −80°C until use.

Stereotaxic injection in mice

Adult mice were anesthetized using isoflurane and analgesia achieved with buprenorphine (0.15 mg/kg) and local scalp administration of lidocaine (5 mg/kg). Once deeply anesthetized, mice were placed into a *Just For Mouse* Stereotaxic Frame with an integrated animal warming base (Stoelting, Wood Dale, IL). Adult C57BL/6 mice (n = 3/group) or adult ChAT(BAC)-eGFP transgenic mice were stereotactically injected into the left mid-striatum at the dose described in the figure legend of each vector preparation in a volume of 2 μL using the following coordinates from bregma in mm: anterior/posterior, AP +0.5; medial/lateral, ML +2.0; dorsal/ventral, DV –2.5. Vectors were infused at a rate of 0.2 μL/min using a Quintessential Stereotaxic Injector pump (Stoelting) to drive a gas-tight Hamilton Syringe (Hamilton, NV) attached to a 10 μL 33G NEUROS model syringe (Hamilton, NV). After injection, the needle was left in place for 2 min to allow the vector solution to disperse and not backflow up the cannula. Buprenorphine (0.15 mg/kg) was injected subcutaneously twice a day for 2 days after the surgery for pain control. The in-life portion of the study is indicated in the figure legends, and it varied from 14 to 16 days.

Immunofluorescence staining and microscopy and image analysis

Mice were deeply anesthetized with an overdose of ketamine/xylazine and transcardially perfused with PBS followed by 4% v/v formaldehyde in 1x PBS. Brains were post-fixed in 4% formaldehyde diluted in PBS for 48 h, followed by 30% (w/v) sucrose for cryopreservation for another 48–72 h after which brains were embedded and frozen in Tissue-Tek O.C.T. compound (Sakura Finetek USA, Torrance, CA). Coronal floating sections (40 μm) were cut using an NX50 CryoStar Cryostat (Thermo Scientific). After rinsing off the sucrose in PBS, the brain sections were treated for immunofluorescence or mounted on glass slides for imaging.

For immunofluorescence, the cryosections were permeabilized with 0.5% v/v Triton X-100 (Millipore Sigma) in PBS for 2 h and blocked with 5% v/v normal goat serum (NGS) in PBS for 1 h. Permeabilization and blocking steps were performed while gently shaking (30 rpm) at room temperature (RT) in 12-well plates. Brain sections with primary antibodies diluted in 1.5% v/v NGS were incubated at 4°C for 24 h on a platform orbital shaker set at 60 rpm. After three washes with PBS, coronal sections and secondary antibodies diluted in 1.5% v/v NGS were incubated for 1 h at RT at 60 rpm. Three PBS washes were performed prior to mounting of stained sections on glass slides for microscopy. Primary antibodies for staining of MSNs were rabbit anti-DARPP32 (ab40801), and the working dilution was 1:100 in 1.5% v/v NGS. Secondary antibodies were goat anti-rabbit Alexa Fluor 350 (Thermo Scientific), and the working dilution was 1:1,000 in 1.5% v/v NGS.

Sections were mounted with Vectashield mounting medium with DAPI (Vector Laboratories, Burlingame, CA), and imaging was performed with a Keyence BZ-X800 microscope (KEYENCE Corporation of America, Itasca, IL) and a NIKON CSU-W1 spinning disk confocal microscope. In the case of imaging the MSNs with anti-DARPP32 and Alexa Fluor 350 antibody, we used mounting media without DAPI to avoid signal overlap.

Image analyses and quantification were performed using the BZ-X100 analyzer software (KEYENCE) for epifluorescence microscope and NIS Elements General Analysis (GA3) for confocal microscope.

For quantitation of spread of transduction of AAV9-CAG-tdTomato and AAV-S-CAG-tdTomato in C57BL/6 mice (n = 3 mice/vector group), we analyzed 11 to 14 sections/mouse spanning 1.5 mm to the rostral and caudal side of the bregma on the ipsilateral injected striatal hemisphere. The area of the injected hemisphere and the transduced region (tdTomato fluorescent positive) within the hemisphere were compared for each section to calculate the percentage of area transduced for each coordinate.

For the quantitation of transduction in ChAT(BAC)-eGFP transgenic mice, six brain sections/mouse (times two mice/group) for AAV9-ChAT-dTomato or AAV-S-ChAT-tdTomato, and 11 brain sections (three to four sections/mouse times three mice/group) from mice injected with AAV9-CAG-tdTomato were imaged using the confocal microscope. Sections were isolated immediately adjacent to the injection site. The images were processed in batches to remove any background noise from the channels. For each section, the entire ipsilateral striatum was selected as the region of interest for quantification. Regions of interest were selected and cropped for further background removal, segmentation, and cell count analysis. The threshold was set accordingly for discriminating among individual cells before counting GFP+ only cells, tdTomato+ only cells, and overlap GFP+/tdTomato+ cells.

Percentages of *in vivo* transduction efficiency of cholinergic neurons were calculated using the number of co-localized (tdTomato+ and ChAT-GFP+) cells divided by the number of ChAT-GFP+ cells and multiplied by 100. Similarly, the percentages of *in vivo* transduction

specificity of cholinergic neurons were calculated using the number of co-localized (tdTomato+ and ChAT-GFP+) cells divided by the number of transduced cells (tdTomato+) in the region of interest. Percentages were calculated for each section of each mouse, and these technical replicates were averaged. Statistical tests were performed using percentages from the biological replicates (individual mice).

Statistics

We used GraphPad Prism 9.0 for PC for statistical analysis. To compare means of two groups, we used an unpaired two-tailed t test; p values < 0.05 were accepted as significant. For comparison of AAV-S and AAV9 transduced area across multiple sections, we used a two-way ANOVA (independent variables were capsid type and region of analysis) followed by a Šídák's multiple comparisons test.

DATA AVAILABILITY

Data are available upon request.

SUPPLEMENTAL INFORMATION

Supplemental information can be found online at https://doi.org/10.1016/j.omtm.2023.05.001.

ACKNOWLEDGMENTS

This work was supported by NIH R01 grant DC017117 and the Collaborative Center for X-linked Dystonia-Parkinsonism Award (to C.A.M.). M.C.S. was partially supported by an American Society of Gene and Cell Therapy Underrepresented Population Fellowship Award in Gene and Cell Therapy. For generation of the artwork in the Figures, BioRender software was utilized for some of the objects. For the AAV capsid cartoons, we used the Protein Data Bank (RCSB PDB) AAV9 capsid structure PDB: http://doi.org/10.2210/pdb7MT0/pdb.[34] We exported the AAV9 structure in 3D viewer into a drawing program for custom coloring. We thank the Molecular Imaging Center MGH Campus Navy Yard (CNY) for their input in the method development for collecting images and quantifying data. We also thank Diane M. Nguyen for assistance with figure artwork.

AUTHOR CONTRIBUTIONS

C.A.M. and M.C.S. conceived of the study, performed experiments, analyzed data, and wrote the manuscript. P.E. performed experiments and analyzed data. M.M. assisted in imaging and quantification analyses and helped write the manuscript. D.D.L.C. and N.P. performed experiments. J.R.S. performed statistical analysis and helped write the manuscript.

DECLARATION OF INTERESTS

C.A.M. has a financial interest in Sphere Gene Therapeutics, Inc., Chameleon Biosciences, Inc., and Skylark Bio, Inc., companies that are developing gene therapy platforms. C.A.M.'s interests were reviewed and are managed by MGH and Mass General Brigham in accordance with their conflict of interest policies. C.A.M. has a filed patent application with claims involving the AAV-S capsid.

REFERENCES

1. Day, J.W., Mendell, J.R., Mercuri, E., Finkel, R.S., Strauss, K.A., Kleyn, A., Tauscher-Wisniewski, S., Tukov, F.F., Reyna, S.P., and Chand, D.H. (2021). Clinical trial and postmarketing safety of onasemnogene abeparvovec therapy. Drug Saf. *44*, 1109–1119.
2. Nathwani, A.C. (2022). Gene therapy for hemophilia. Hematology. Am. Soc. Hematol. Educ. Program *2022*, 569–578.
3. Gruntman, A.M., and Flotte, T.R. (2018). The rapidly evolving state of gene therapy. Faseb. J. *32*, 1733–1740.
4. Tai, C.H., Lee, N.C., Chien, Y.H., Byrne, B.J., Muramatsu, S.I., Tseng, S.H., and Hwu, W.L. (2022). Long-term efficacy and safety of eladocagene exuparvovec in patients with AADC deficiency. Mol. Ther. *30*, 509–518.
5. Kravitz, A.V., and Kreitzer, A.C. (2012). Striatal mechanisms underlying movement, reinforcement, and punishment. Physiology *27*, 167–177.
6. Simpson, E.H., Kellendonk, C., and Kandel, E. (2010). A possible role for the striatum in the pathogenesis of the cognitive symptoms of schizophrenia. Neuron *65*, 585–596.
7. Piggott, M.A., Marshall, E.F., Thomas, N., Lloyd, S., Court, J.A., Jaros, E., Burn, D., Johnson, M., Perry, R.H., McKeith, I.G., et al. (1999). Striatal dopaminergic markers in dementia with Lewy bodies, Alzheimer's and Parkinson's diseases: rostrocaudal distribution. Brain *122*, 1449–1468.
8. Kita, H., and Kitai, S.T. (1988). Glutamate decarboxylase immunoreactive neurons in rat neostriatum: their morphological types and populations. Brain Res. *447*, 346–352.
9. Oldenburg, I.A., and Ding, J.B. (2011). Cholinergic modulation of synaptic integration and dendritic excitability in the striatum. Curr. Opin. Neurobiol. *21*, 425–432.
10. Castle, M.J., Cheng, Y., Asokan, A., and Tuszynski, M.H. (2018). Physical positioning markedly enhances brain transduction after intrathecal AAV9 infusion. Sci. Adv. *4*, eaau9859.
11. Martel, A.C., Elseedy, H., Lavigne, M., Scapula, J., Ghestem, A., Kremer, E.J., Esclapez, M., and Apicella, P. (2020). Targeted transgene expression in cholinergic interneurons in the monkey striatum using canine adenovirus serotype 2 vectors. Front. Mol. Neurosci. *13*, 76.
12. Tallini, Y.N., Shui, B., Greene, K.S., Deng, K.Y., Doran, R., Fisher, P.J., Zipfel, W., and Kotlikoff, M.I. (2006). BAC transgenic mice express enhanced green fluorescent protein in central and peripheral cholinergic neurons. Physiol. Genom. *27*, 391–397.
13. Gamage, R., Zaborszky, L., Münch, G., and Gyengesi, E. (2023). Evaluation of eGFP expression in the ChAT-eGFP transgenic mouse brain. BMC Neurosci. *24*, 4.
14. Hanlon, K.S., Meltzer, J.C., Buzhdygan, T., Cheng, M.J., Sena-Esteves, M., Bennett, R.E., Sullivan, T.P., Razmpour, R., Gong, Y., Ng, C., et al. (2019). Selection of an efficient AAV vector for robust CNS transgene expression. Mol. Ther. Methods Clin. Dev. *15*, 320–332.
15. Ivanchenko, M.V., Hanlon, K.S., Hathaway, D.M., Klein, A.J., Peters, C.W., Li, Y., Tamvakologos, P.I., Nammour, J., Maguire, C.A., and Corey, D.P. (2021). A versatile capsid variant for transduction of mouse and primate inner ear. Mol. Ther. Methods Clin. Dev. *21*, 382–398.
16. Bausero, P., Schmitt, M., Toussaint, J.L., Simoni, P., Geoffroy, V., Queuche, D., Duclaud, S., Kempf, J., and Quirin-Stricker, C. (1993). Identification and analysis of the human choline acetyltransferase gene promoter. Neuroreport *4*, 287–290.
17. Perez, B.A., Shutterly, A., Chan, Y.K., Byrne, B.J., and Corti, M. (2020). Management of neuroinflammatory responses to AAV-mediated gene therapies for neurodegenerative diseases. Brain Sci. *10*, 119.
18. Syková, E., and Nicholson, C. (2008). Diffusion in brain extracellular space. Physiol. Rev. *88*, 1277–1340.
19. Jang, J.H., Schaffer, D.V., and Shea, L.D. (2011). Engineering biomaterial systems to enhance viral vector gene delivery. Mol. Ther. *19*, 1407–1415.
20. Lonser, R.R., Akhter, A.S., Zabek, M., Elder, J.B., and Bankiewicz, K.S. (2020). Direct convective delivery of adeno-associated virus gene therapy for treatment of neurological disorders. J. Neurosurg. *134*, 1751–1763.
21. Bankiewicz, K.S., Eberling, J.L., Kohutnicka, M., Jagust, W., Pivirotto, P., Bringas, J., Cunningham, J., Budinger, T.F., and Harvey-White, J. (2000). Convection-enhanced delivery of AAV vector in parkinsonian monkeys; in vivo detection of gene expression and restoration of dopaminergic function using pro-drug approach. Exp. Neurol. *164*, 2–14.

22. Hadaczek, P., Kohutnicka, M., Krauze, M.T., Bringas, J., Pivirotto, P., Cunningham, J., and Bankiewicz, K. (2006). Convection-enhanced delivery of adeno-associated virus type 2 (AAV2) into the striatum and transport of AAV2 within monkey brain. Hum. Gene Ther. *17*, 291–302.

23. Kaspar, B.K., Erickson, D., Schaffer, D., Hinh, L., Gage, F.H., and Peterson, D.A. (2002). Targeted retrograde gene delivery for neuronal protection. Mol. Ther. *5*, 50–56.

24. Ciesielska, A., Mittermeyer, G., Hadaczek, P., Kells, A.P., Forsayeth, J., and Bankiewicz, K.S. (2011). Anterograde axonal transport of AAV2-GDNF in rat basal ganglia. Mol. Ther. *19*, 922–927.

25. Haggerty, D.L., Grecco, G.G., Reeves, K.C., and Atwood, B. (2020). Adeno-associated viral vectors in neuroscience research. Mol. Ther. Methods Clin. Dev. *17*, 69–82.

26. Castle, M.J., Perlson, E., Holzbaur, E.L., and Wolfe, J.H. (2014). Long-distance axonal transport of AAV9 is driven by dynein and kinesin-2 and is trafficked in a highly motile Rab7-positive compartment. Mol. Ther. *22*, 554–566.

27. Gehrlach, D.A., Weiand, C., Gaitanos, T.N., Cho, E., Klein, A.S., Hennrich, A.A., Conzelmann, K.K., and Gogolla, N. (2020). A whole-brain connectivity map of mouse insular cortex. Elife *9*, e55585.

28. Albin, R.L., Minderovic, C., and Koeppe, R.A. (2017). Normal striatal vesicular acetylcholine transporter expression in tourette syndrome. eNeuro *4*. ENEURO.0178-17.2017.

29. Xu, M., Kobets, A., Du, J.C., Lennington, J., Li, L., Banasr, M., Duman, R.S., Vaccarino, F.M., DiLeone, R.J., and Pittenger, C. (2015). Targeted ablation of cholinergic interneurons in the dorsolateral striatum produces behavioral manifestations of Tourette syndrome. Proc. Natl. Acad. Sci. USA *112*, 893–898.

30. Pasquini, J., Brooks, D.J., and Pavese, N. (2021). The cholinergic brain in Parkinson's disease. Mov. Disord. Clin. Pract. *8*, 1012–1026.

31. Earley, L.F., Conatser, L.M., Lue, V.M., Dobbins, A.L., Li, C., Hirsch, M.L., and Samulski, R.J. (2020). Adeno-associated virus serotype-specific inverted terminal repeat sequence role in vector transgene expression. Hum. Gene Ther. *31*, 151–162.

32. Hordeaux, J., Buza, E.L., Jeffrey, B., Song, C., Jahan, T., Yuan, Y., Zhu, Y., Bell, P., Li, M., Chichester, J.A., et al. (2020). MicroRNA-mediated inhibition of transgene expression reduces dorsal root ganglion toxicity by AAV vectors in primates. Sci. Transl. Med. *12*, eaba9188.

33. Ivanchenko, M.V., Hanlon, K.S., Devine, M.K., Tenneson, K., Emond, F., Lafond, J.F., Kenna, M.A., Corey, D.P., and Maguire, C.A. (2020). Preclinical testing of AAV9-PHP.B for transgene expression in the non-human primate cochlea. Hear. Res. *394*, 107930.

34. Penzes, J.J., Chipman, P., Bhattacharya, N., Zeher, A., Huang, R., McKenna, R., and Agbandje-McKenna, M. (2021). Adeno-associated virus 9 structural rearrangements induced by endosomal trafficking pH and glycan attachment. J. Virol. *95*, e0084321.